

RESEARCH ARTICLE



## *Astragalus* polysaccharide (APS) attenuated PD-L1-mediated immunosuppression via the miR-133a-3p/MSN axis in HCC

Lihua He<sup>a</sup>, Kecheng Xu<sup>b</sup>, Lizhi Niu<sup>b</sup> and Lizhu Lin<sup>c</sup>

<sup>a</sup>Department of Oncology, Guangzhou University of Traditional Chinese Medicine, Guangzhou, China; <sup>b</sup>Department of Oncology, Fuda Cancer Hospital, Guangzhou, China; <sup>c</sup>Division of Oncology, First Affiliated Hospital, Guangzhou University of Chinese Medicine, Guangzhou, China

### ABSTRACT

**Context:** *Astragalus* polysaccharide (APS) is a new tumour therapeutic drug, that has an inhibitory effect on a variety of solid tumours. Tumour cell immunosuppression is related to the up-regulation of programmed death ligand 1 (PD-L1). However, whether APS exerts its antitumor effect by regulating PD-L1 remains unclear.

**Objective:** To explore whether APS exerts its antineoplastic effect via regulating PD-L1-mediated immunosuppression in hepatocellular carcinoma (HCC).

**Materials and methods:** SMMC-7721 cells were subcutaneous injected into BALB/C mice for HCC model establishment. Mice were intraperitoneally injected with 100, 200 and 400 mg/kg APS for 12 days. Immunohistochemistry (IHC) was performed to assess CD8<sup>+</sup> T cells' rate and PD-L1 level in HCC tissues. HCC cells were pre-treated with 0.1, 0.5 and 1 mg/mL APS for 4 h, then were treated with 10 ng/mL IFN- $\gamma$  24 h. PD-L1 level and cell apoptosis was detected by flow cytometry. PD-L1 and Moesin (MSN) proteins were measured by western blot. MiR-133a-3p and MSN mRNA levels were assessed by qRT-PCR. The targets of miR-133a-3p were predicted by starBase, and which was verified by dual-luciferase reporter assay.

**Results:** Our findings illustrated that APS dose-dependently inhibited HCC growth tested with IC<sub>50</sub> values of 4.2 mg/mL, and IFN- $\gamma$ -induced PD-L1 expression and attenuated PD-L1-mediated immunosuppression in HCC cells. APS attenuated PD-L1-mediated immunosuppression via miR-133a-3p in HCC cells. Besides, miR-133a-3p targeted to MSN, and MSN inhibited the antitumor effect of APS by maintaining the stability of PD-L1. Moreover, APS attenuated PD-L1-mediated immunosuppression via the miR-133a-3p/MSN axis.

**Conclusions:** APS attenuated PD-L1-mediated immunosuppression via miR-133a-3p/MSN axis to develop an antitumor effect. APS may be an effective drug for HCC treatment.

### ARTICLE HISTORY

Received 31 March 2022  
Revised 3 August 2022  
Accepted 9 August 2022

### KEYWORDS

Hepatocellular carcinoma;  
*Astragalus* polysaccharide;  
moesin

### Introduction

Hepatocellular carcinoma (HCC) is responsible for the third most common cancer-related death worldwide (Ince et al. 2020). Researches showed that there are many factors that cause HCC, such as HBV and the coronavirus disease 2019 (COVID-19) (Baskiran et al. 2020; Akbulut et al. 2022). Moreover, HCC is a common malignant tumour with high morbidity and mortality (Chen et al. 2020). With the continuous improvement of medical care, the treatment of HCC has made some progress, but the 5-year survival rate of patients remains less than ideal. HCC seriously affects human health and brings huge economic burden. Moreover, HCC is an insidious tumour that is often diagnosed in a later stage of life. The tumour microenvironment is the key to tumorigenesis and progression. Many cellular and non-cellular components orchestrate the intricate process of hepatocarcinogenesis. The most important feature of hepatocellular cancer is the immune evasion process (Huang et al. 2020; Ince et al. 2020; Satilmis et al. 2021). It is reported that the expression pattern of programmed death-1 ligand 1 (PD-L1) in tumour cells or monocyte/macrophage (Mo/M $\phi$ s) is a predictive biomarker of HCC

patients (Kudo 2020). Furthermore, studies indicated that in the tumour microenvironment, PD-L1 is regulated via interferon- $\gamma$  (IFN- $\gamma$ ). For example, IFN- $\gamma$  produced by tumour infiltrating lymphocytes (TIL) activate the AK/STAT pathway by activating the receptor, and eventually modulate PD-L1 expression through the activated JAK/STAT pathway (Blank et al. 2004; Spranger et al. 2013). In short, PD-L1 mediated immunosuppression has been confirmed. Therefore, to explore drugs that reduce IFN- $\gamma$ -induced PD-L1 expression can effectively restore the function of killer T cells, which is expected to contribute to the immunotherapy of HCC. *Astragalus* polysaccharide (APS) is the main compound derived from the genus *Astragalus* commonly used in many herbal formulations, which is widely used to treat a variety of diseases (Auyeung et al. 2016). It is reported that APS has a variety of functions, including immunomodulatory and antitumor functions. Yang et al. (2020) demonstrated that APS inhibits breast cancer progression through the Wnt/ $\beta$ -catenin pathway. In pancreatic cancer, APS exerts its antitumor effect by reducing the levels of AKT, ERK and MMP-9 (Wu et al. 2018). Furthermore, APS plays an antitumor role via regulating the secretion of cytokines to regulate the immune system

**CONTACT** Lizhu Lin  [Lizhulin26@yahoo.com](mailto:Lizhulin26@yahoo.com)  Division of Oncology, First Affiliated Hospital, Guangzhou University of Chinese Medicine, No.16, JichangRoad, Guangzhou 510504, Guangdong Province, P.R. China

 Supplemental data for this article can be accessed online at <https://doi.org/10.1080/13880209.2022.2112963>.

© 2022 The Author(s). Published by Informa UK Limited, trading as Taylor & Francis Group.

This is an Open Access article distributed under the terms of the Creative Commons Attribution-NonCommercial License (<http://creativecommons.org/licenses/by-nc/4.0/>), which permits unrestricted non-commercial use, distribution, and reproduction in any medium, provided the original work is properly cited.

(Li et al. 2020). In lung adenocarcinoma, APS reverses epithelial-mesenchymal transition through the PD-L1/SREBP-1/EMT signal pathway (Wei et al. 2020). Hwang et al. (2021) suggest that APS serves as a local sticky adjuvant to improve the anticancer effect of PD-L1 immune checkpoint inhibitors. Although the mechanism of antitumor effect of APS by regulating PD-L1 expression has been preliminarily reported, whether APS plays an antitumor effect through PD-L1 in HCC remains unclear.

As is well-known, the human genome contains a large number of non-coding sequences, which can be divided into microRNA (miRNAs) with a length of about 18-22 bp and long non-coding RNAs (lncRNAs) greater than 200 bp in length (Nallasamy et al. 2018). The 3' untranslated regions (3'-UTR) of mRNA was bound by miRNAs to participate in the post-transcriptional regulation of many genes (Ding et al. 2020). It is reported that a large number of miRNAs are involved in the regulation of HCC progression, including miR-15b-5p, miR-338-5p and miR-764, etc. (Chen et al. 2015). Furthermore, the mechanism of miRNAs regulating tumour immunosuppression by regulating PD-L1 has been elucidated preliminarily. Cristino et al. (2019) reported that miR-BHRF1-2-5p binds PD-L1 and PD-L2 3'-UTR reducing PD-L1/L2 and attenuating immunosuppression in diffuse large B-cell lymphoma (DLBCLs). MiR-let-7 inactivates CD8<sup>+</sup> T cells via regulating PD-L1 to contribute to immune escape of NSCLC cells (Zhao et al. 2019). MiR-133a-3p's mechanism of action in tumours has also been widely reported, including oral squamous cell carcinoma (OSCC), prostate cancer, and HCC (He et al. 2018; Liang et al. 2018; Tang et al. 2018). Liang et al. (2018) showed that miR-133a-3p was decreased in HCC and serves as a vital marker for the diagnosis of hepatocellular carcinoma. Han et al. (2020) found that miR-133a-3p regulates HCC progression by targeting CORO1C. In total, the mechanism of miRNAs regulating tumour immunosuppression by regulating PD-L1 has been elucidated preliminarily, and miR-133a-3p was decreased in HCC and serves as a vital marker for the diagnosis of HCC. However, whether miR-133a-3p participates in PD-L1-mediated immunosuppression of HCC remains unclear.

As an important member of the ezrin, radixin and Moesin (MSN) families, MSN participates in the regulation of cell surface structure and specific membrane domains (Fehon et al. 2010). It is reported that MSN exists not only in the cell membrane and cytoplasm, but also in the nucleus, which is closely related to the fact that MSN promotes breast cancer development (Qin et al. 2020). Increasing evidence shows that overexpressed MSN is related to tumour metastasis and poor prognosis in tumour patients. Barros et al. (2018) showed that MSN is up-regulated in oral cancer and served as a prognostic marker or therapeutic target. MSN expression in pancreatic carcinoma was related to tumour pathological stage, nerve infiltration and pain degree of tumour site (Liang et al. 2019). However, role and its underlying mechanism of MSN in HCC remains unclear. Furthermore, Meng et al. (2020) indicated that MSN is necessary for the stability of PD-L1 in breast cancer. Moreover, at the beginning of the study, starBase was applied to predict the downstream targets of miR-133a-3p. Results showed that there was a binding site between miR-133a-3p and MSN. Therefore, we explored whether miR-133a-3p participates in PD-L1-mediated immunosuppression of HCC by targeting MSN. Previous findings suggest that APS plays an antitumor effect via regulating PD-L1. However, whether miR-133a-3p regulates PD-L1-mediated immunosuppression to exert antitumor effect remains unclear. In this paper, we hypothesised that APS attenuated PD-

L1-mediated immunosuppression via the miR-133a-3p/MSN axis in HCC. We clarified the potential mechanism of antitumor effect of APS in HCC.

## Materials and methods

### Animal model

SMMC-7721 cells ( $1 \times 10^6$  cells per mouse, Peking Union Cell Bank, Beijing, China) were injected into BALB/C mice through subcutaneous injection for HCC model establishment. Following 24 h, HCC BALB/C mice were divided into 4 groups ( $n=6$ ). Control group, HCC BALB/C mice were untreated; APS groups, HCC BALB/C mice were injected with APS 100, 200 and 400 mg/kg (Sigma Chemicals), respectively. BALB/C mice were injected continuously for 12 days, and the tumour size was recorded every three days. After 12 d, BALB/C mice were sacrificed by cervical dislocation and the tumour was removed for statistics of tumour size, weight and volume.

### PBMCs-mediated tumour cell killing

Human peripheral blood mononuclear cells (PBMCs) were purchased from ORIBIOTECH (Shanghai, China). 12-well plates were used to culture SMMC-7721 or Huh-7 cells with a density of  $1 \times 10^5$  cells per well. PBMCs were activated by co-culturing with 2  $\mu$ g/mL CD3 antibody (Abcam, Cambridge, UK) and 1  $\mu$ g/mL CD28 antibody (Abcam) for 24 h. Then the activated PBMCs was incubated with SMMC-7721 or Huh-7 cells with the proportion of 5:1 of for 72 h. Annexin V and propidium iodide were stained. Finally, SMMC-7721 or Huh-7 cells were used to analyse the apoptosis rate by flow cytometry.

### Conditioned medium (CM) from PBMCs

Activated PBMCs-CM were collected and centrifuged. The cell fragments were removed and the supernatant was filtered with 0.22  $\mu$ m disposable polyvinylidene fluoride (PVDF) membrane (Thermo Fisher Science, Waltham, MA, USA). The CM from inactivated PBMCs was also collected.

### Immunohistochemistry

First, 4- $\mu$ m-thick HCC tissue sections were formalin-fixed and paraffin-embedded. Tissue sections were rehydrated with graded ethanol, treated with 3% hydrogen peroxide and methanol for 10 min to inhibit endogenous peroxidase, and then treated in the microwave oven for 10 min for antigen retrieval. Then the sections were incubated with normal goat serum at 37°C for 30 min, and rabbit anti-CD8 and anti-PD-L1 antibodies (Abcam, Cambridge, UK, 1:500) were incubated at 37°C for 1 h. Besides, sections were incubated with 1:100 dilution of biotin-labeled sheep anti-rabbit immunoglobulin secondary antibody at 37°C for 1 h. Finally, colour was developed in 3,3'-diaminobenzidine tetrachloride (Abcam, Cambridge, UK).

### Cell culture

293T cells and HCC cells including SMMC-7721 and Huh-7 cells were provided by Peking Union Cell Bank (Beijing, China), cultivated within DMEM (Thermo Fisher Scientific, Waltham, MA, USA) that contained 10% FBS (Gibico, NY, USA) and incubated

within the humid incubator under 37°C and 5% CO<sub>2</sub> conditions.

### Cell transfection

MSN (wild type-MSN, phosphorylated T558D-MSN), miR-133a-3p inhibitor, miR-133a-3p mimic, sh-MSN vector, and negative controls (NC inhibitor, NC mimic and sh-NC vector) were synthesised by GeneChem (Shanghai, China). SMMC-7721 and Huh-7 were seeded in 6-well cell culture dishes overnight in serum-free medium. On the second day, after washing the cells with PBS, Lipofectamine 3000 reagent (Invitrogen, CA, USA) was used to transfect corresponding plasmids, based on the instructions. For 24 h transfection, HCC cells were used in subsequent experiments. Besides, HCC cells including SMMC-7721 and Huh-7 cells were respectively pre-treated with 0.1 mg/mL, 0.5 mg/mL and 1 mg/mL of APS (Chun Test Biotechnology Co., LTD, Shanghai, China) for 4 h, then APS-treated cells were treated with 10 ng/mL IFN- $\gamma$  (Baiolaibo Technology Co., LTD, Beijing, China) for 24 h.

### Flow cytometry

Activated PBMCs were incubated with SMMC-7721 or Huh-7 cells with the proportion of 5:1 of for 72 h. Subsequently, treated HCC cells including SMMC-7721 and Huh-7 cells were isolated by Transwell. The cell suspension containing  $1 \times 10^5$  cells were fixed in precooled 2% frozen formaldehyde. Subsequently, HCC coupled with fluorescein isothiocyanate (FITC) (Beyotime, Nanjing, China) was incubated with anti-PD-L1 for 30 min. Finally, FACS Calibur system (BD Biosciences, NY, USA) was used for flow cytometry, and Cellquest graphics software was used to collect and analyse data.

### Western blot

HCC cells were cleaved with RIPA cleavage buffer to extract total protein. The BCA method was used to quantify total protein. Subsequently, the total protein (20  $\mu$ g) was separated by 10% SDS-PAGE and the protein was electroprinted on PVDF membrane. The PVDF membrane was incubated with rabbit anti-MSN, anti-p-MSN and anti-PD-L1 antibodies (Abcam, Cambridge, UK, 1:1000) overnight at 4°C. On the 2<sup>nd</sup> day, the second anti-rabbit IgG antibody coupled with HRP was incubated for 2 h, and the bands were detected by immobilised Western chemiluminescence instrument.  $\beta$ -Tubulin was used as the endogenous control. Finally, ImageJ software was used to quantify the strength of the bands obtained from Western blot analysis.

### qRT-PCR

TRIzol reagent (Invitrogen, California, USA) was used to extract total RNA; miRNAs in serum were collected by mirVana microRNA Isolation kits (Invitrogen). miR-133a-3p level was detected by Taqman microRNA assay kit (Invitrogen). U6 RNA was used as the endogenous control in data analysis. One-Step SYBR Prime Script PLUS RT-PCR kit (Invitrogen) was used to detect the levels of MSN gene. GAPDH was used as the endogenous control in data analysis. Finally, fold changes were calculated using the  $2^{-\Delta\Delta Ct}$  method. The entire process was

**Table 1.** The gene primer sequences used for qRT-PCR.

Gene	Forward (5'→3')	Reverse (5'→3')
miR-133a-3p	GCCTTGGTCCCCTTCAAC	TATGCTTGTTCTCGTCTCTGTGC
MSN	ATCACTCAGCGCTGTCTT	CCCACTGGTCTTGTGAGT
U6	ATTGGAACGATACAGAGAAGATT	GGAACGCTTCACGAATTTG
GAPDH	CCAGTGGTCTCTCTGA	GCTGTAGCCAAATCGTTGT

repeated three times. The primers used in this study are listed in Table 1.

### CO-IP assay

Cells were lysed by freeze-lytic buffer (Beyotime, Nanjing, China) for 30 min and centrifuged (1,500 g) at 4°C for 15 min. The upper layer was incubated with antibodies for 1 h at 4°C. Subsequently, the protein mixture was incubated on a bead (Marge Fisher Scientific, USA) at 4°C for 2 h and washed twice with 1 mL of lysis buffer. Then, 20  $\mu$ L of 2 $\times$  SDS buffer was added for elution. Analysis was performed by Western blotting after centrifugation.

### miR-133a-3p target selection and dual-luciferase reporter assay

Firstly, the potential binding sites of miR-133a-3p downstream was predicted by using starBase. Dual-luciferase reporter assay was conducted to confirm the physical interaction between miR-133a-3p and MSN. In detail, mutant type (MUT) MSN or wild type (WT) MSN was subcloned to pGL3 luciferase reporter vectors (Promega, Madison, WI, USA) to construct MSN-WT and MSN-MUT. Subsequently, HCC cells were co-transfected with MSN-WT or MSN-MUT and miR-133a-3p mimics or mimics NC by Lipofectamine<sup>TM</sup>3000 (Takara, Dalian, China). Following 48 h, luciferase activity was detected.

### Statistical analysis

Data from at least 3 replicates were presented as mean  $\pm$  standard deviation (SD). Two groups were compared using Student's *t*-test, and multiple groups were compared using one-way ANOVA and Tukey's multiple comparison test.  $P < 0.05$  means the difference was statistically significant.

## Results

### APS inhibited HCC growth and attenuated PD-L1-mediated immunosuppression

HCC model of BALB/C mice was established, and HCC BALB/C mice were treated with APS 100, 200, and 400 mg/kg, respectively. After 12 days, statistical analysis of tumour size, weight and volume indicated that APS inhibited the size, weight and volume of tumour in a dose-dependent manner (Figure 1A–C). Subsequently, IHC analysis showed that with the increase of APS concentration, the number of CD8<sup>+</sup>T cells was increased, while PD-L1 expression was decreased (Figure 1D and E). Moreover, the effect of APS on the viability of normal hepatocytes LO2 cells was detected. Results showed that the dose in the experiment had no significant effect on LO2 cells (Figure S1). These findings suggest that APS inhibited HCC growth and attenuated PD-L1-mediated immunosuppression.

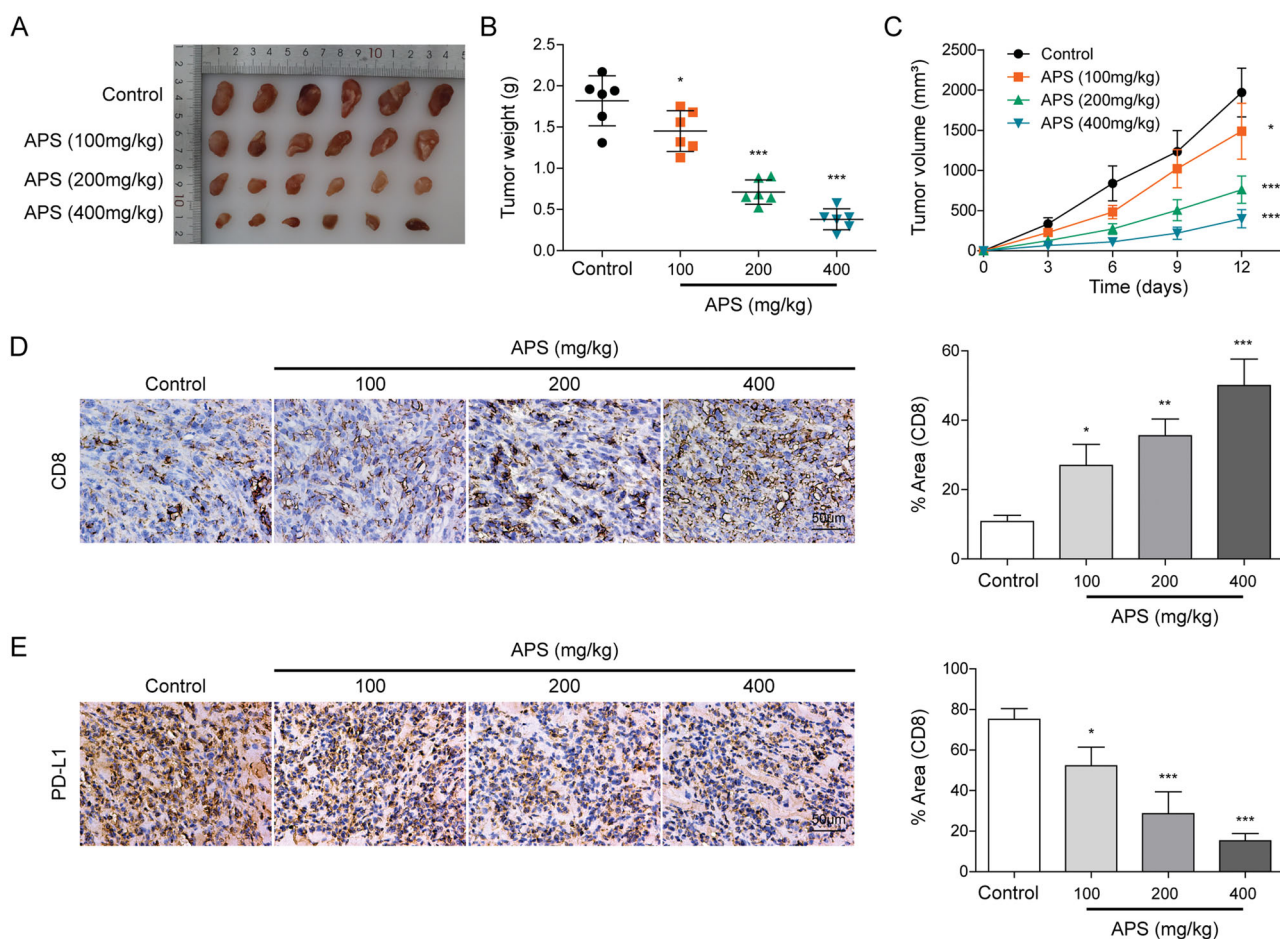


**Figure 1.** APS inhibited HCC growth and attenuated PD-L1-mediated immunosuppression. (A) Morphological observation of tumours. (B and C) Statistical analysis of tumour weight and volume. (D) CD8<sup>+</sup> cells infiltration was detected by IHC. (E) PD-L1 level was detected by IHC. The data were expressed as mean  $\pm$  SD. All data were obtained from at least three replicate experiments ( $n = 6$ ). \* $P < 0.05$ , \*\*\* $P < 0.001$ .

### APS inhibited IFN- $\gamma$ -induced PD-L1 expression and attenuated PD-L1-mediated immunosuppression

HCC cells including SMMC-7721 and Huh-7 cells were respectively pre-treated with (0.1, 0.5 and 1 mg/mL) APS for 4 h, then APS-treated cells were furtherly treated with 10 ng/mL IFN- $\gamma$  for 24 h. Flow cytometry analysis indicated that IFN- $\gamma$  induced PD-L1 expression in HCC cells surface, while APS antagonised PD-L1 expression in a dose-dependent manner (Figure 2A and B). Similarly, CM<sup>+</sup> induced PD-L1 expression in HCC cells surface, whereas APS reversed PD-L1 expression in a dose-dependent manner (Figure 2C and D). Consistently, results showed that PD-L1 expression induced by IFN- $\gamma$  was inhibited by APS in a dose-dependent manner on HCC cell (Figure 2E and F). Finally, functional researches showed that IFN- $\gamma$  promoted PD-L1 expression on the surface of tumour cells and reduced the sensitivity of tumour cells to cytotoxicity mediated by PBMCs, whereas APS alleviated IFN- $\gamma$  effect (Figure 2G and H). Taken together, APS inhibited IFN- $\gamma$ -induced PD-L1 expression and attenuated PD-L1-mediated immunosuppression.

### APS attenuated PD-L1-mediated immunosuppression via miR-133a-3p

The regulatory role of miR-133a-3p in HCC progression has been reported (Liang et al. 2018; Han et al. 2020). To further

explore whether APS plays an immunomodulatory role via miR-133a-3p in HCC, SMMC-7721 and Huh-7 cells were respectively pre-treated with 0.1 mg/mL, 0.5 mg/mL, and 1 mg/mL of APS for 4 h, and APS-treated cells were treated with 10 ng/mL IFN- $\gamma$  for 24 h. Results indicated that miR-133a-3p expression inhibited by IFN- $\gamma$  was alleviated by APS in a dose-dependent manner in HCC cells (Figure 3A). Subsequently, miR-133a-3p inhibitor was transfected into SMMC-7721 and Huh-7 cells for miR-133a-3p inhibition, NC inhibitor served as the negative control. Results showed that miR-133a-3p expression was significantly decreased by miR-133a-3p inhibitor (Figure 3B). Flow cytometry analysis showed that PD-L1 expression was induced by IFN- $\gamma$  on HCC cells surface, and APS antagonised the IFN- $\gamma$  effect whereas the effect of APS was alleviated by miR-133a-3p inhibition (Figure 3C and D). Consistently, PD-L1 expression detected by Western blot was consistent with that of flow cytometry (Figure 3E and F). Furthermore, activated PBMCs cells were co-cultured with treated SMMC-7721 and Huh-7 cells at 5:1 for 72 h, SMMC-7721 and Huh-7 cells were isolated and collected. Functionally, IFN- $\gamma$  induced PD-L1 expression caused a decreased tumour cell sensitivity to PBMCs-mediated cytotoxicity, but the effect of IFN- $\gamma$  was alleviated by APS, and APS effect was reversed by miR-133a-3p inhibition (Figure 3G and H). These findings suggest that APS attenuated PD-L1-mediated immunosuppression via miR-133a-3p.

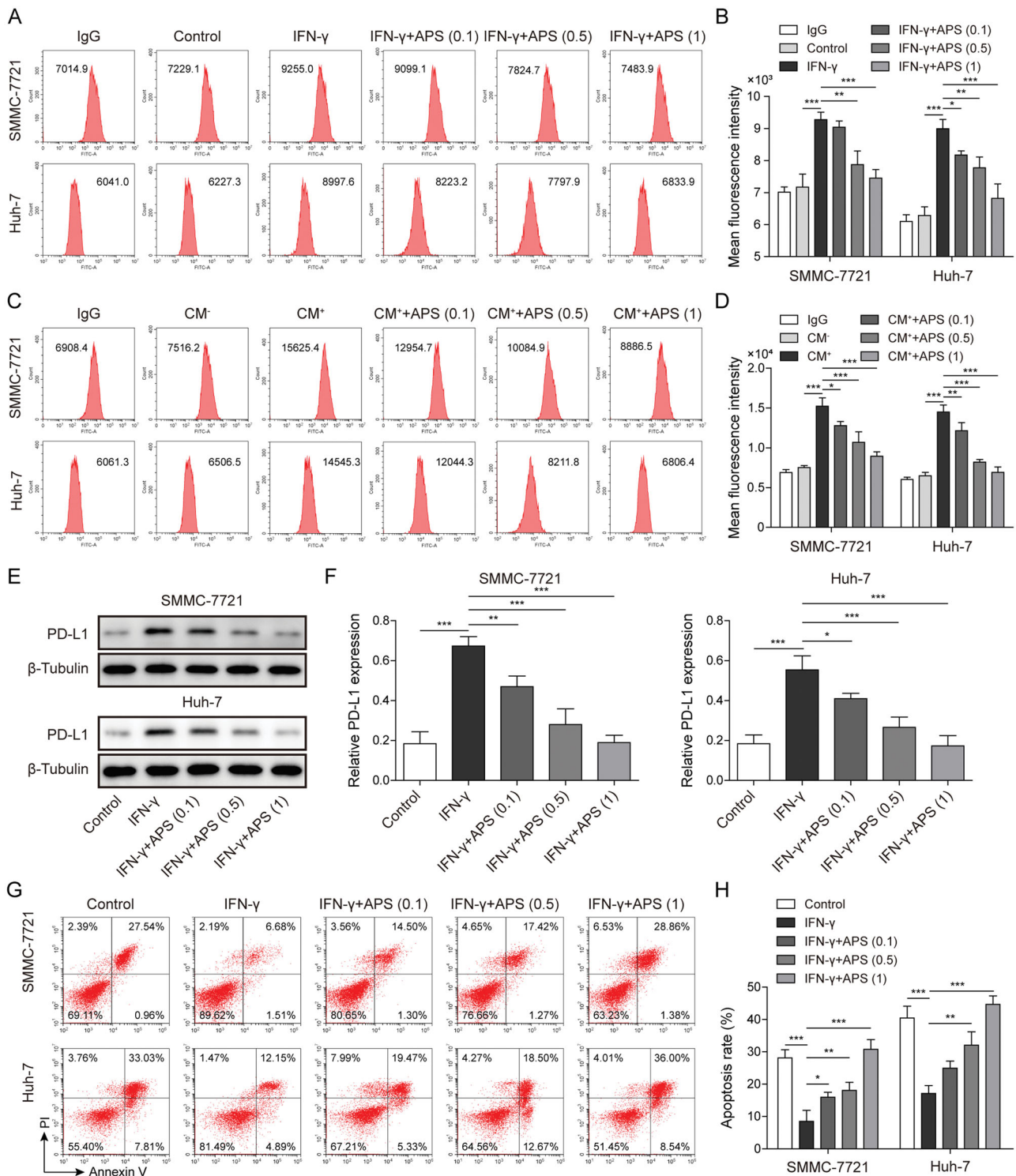


**Figure 2.** APS inhibited IFN- $\gamma$ -induced PD-L1 expression and attenuated PD-L1-mediated immunosuppression. HCC cells including SMMC-7721 and Huh-7 cells were respectively pre-treated with 0.1 mg/mL, 0.5 mg/mL and 1 mg/mL of APS for 4 h, then APS-treated cells were treated with 10 ng/mL IFN- $\gamma$  for 24 h. (A–D) The level of PD-L1 on SMMC-7721 and Huh-7 cells surface was detected by flow cytometry. (E and F) PD-L1 protein level on SMMC-7721 and Huh-7 cells surface was measured by Western blot. (G and H) Activated PBMCs cells were co-cultured with treated SMMC-7721 and Huh-7 cells at 5:1 for 72 h, SMMC-7721 and Huh-7 cells were isolated and collected. PBMCs mediated-HCC cell killing effect was detected by flow cytometry. The data were expressed as mean  $\pm$  SD. All data were obtained from at least three replicate experiments ( $n = 3$ ). \* $P < 0.05$ , \*\* $P < 0.01$ , \*\*\* $P < 0.001$ .

### MSN served as a target for miR-133a-3p

Studies showed that miR-133a-3p participates in the regulation of HCC progression by targeting genes (Han et al. 2020). qRT-PCR analysis indicated that MSN level was induced by IFN- $\gamma$ , while APS antagonised the high expression of MSN in a

dose-dependent manner (Figure 4A). Subsequently, miR-133a-3p inhibitor or miR-133a-3p mimic was transfected into SMMC-7721 and Huh-7 cells for miR-133a-3p inhibition or overexpression, NC inhibitor or mimic served as the negative control. Results showed that MSN expression was significantly inhibited

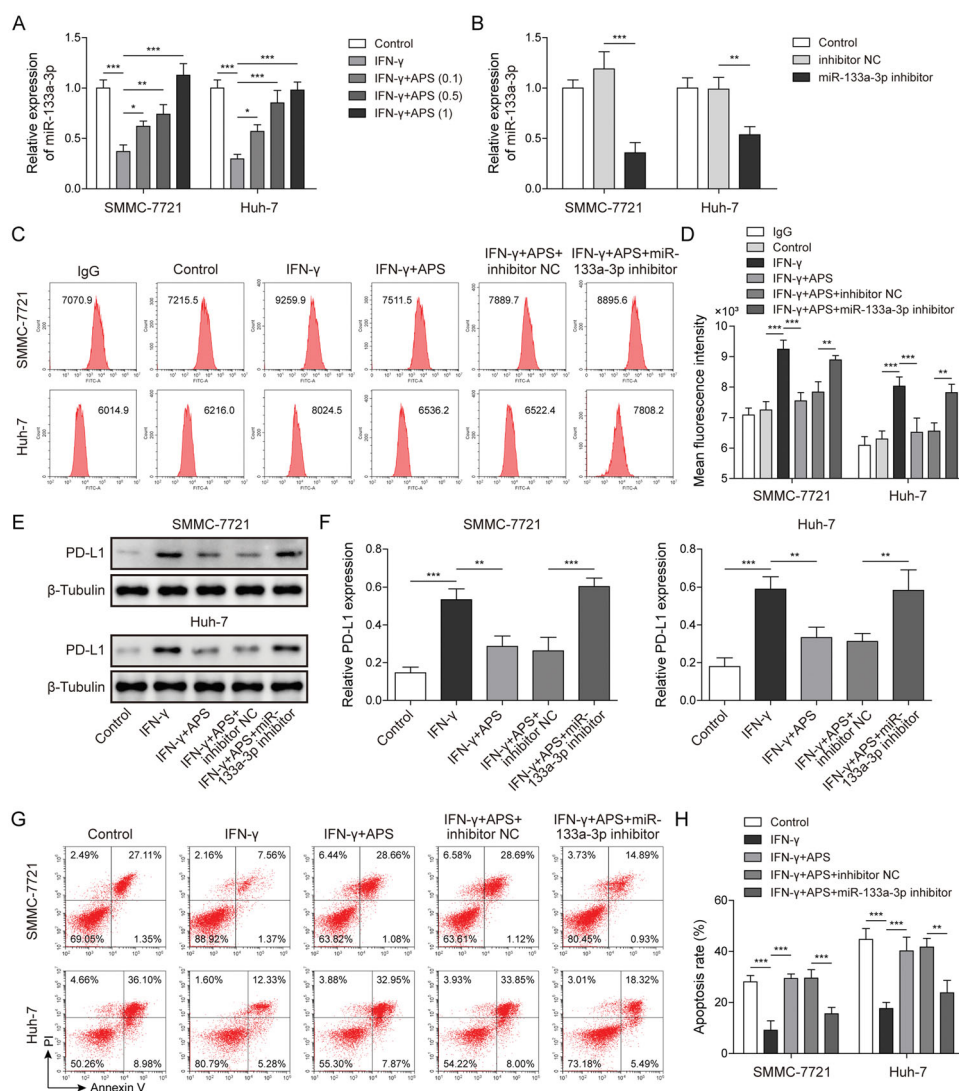


**Figure 3.** APS attenuated PD-L1-mediated immunosuppression via miR-133a-3p. (A and B) miR-133a-3p level was detected by qRT-PCR. (C and D) PD-L1 level on SMMC-7721 and Huh-7 cells surface was detected by flow cytometry. (E and F) PD-L1 protein level on SMMC-7721 and Huh-7 cells surface was detected by Western blot. (G and H) Activated PBMCs cells were co-cultured with treated SMMC-7721 and Huh-7 cells at 5:1 for 72 h, SMMC-7721 and Huh-7 cells were isolated and collected. SMMC-7721 and Huh-7 cells' apoptosis was evaluated by flow cytometry. The data were expressed as mean  $\pm$  SD. All data were obtained from at least three replicate experiments ( $n = 3$ ). \* $P < 0.05$ , \*\* $P < 0.01$ , \*\*\* $P < 0.001$ .

by miR-133a-3p overexpression, whereas miR-133a-3p inhibition significantly increased MSN expression (Figure 4B and C). Furthermore, a binding site between miR-133a-3p and MSN mRNA was predicted by starBase, and dual-luciferase reporter assay analysis revealed that the luciferase activity of MSN-WT reported gene was inhibited by co-transfection of miR-133a-3p mimics, but the co-transfection of miR-133a-3p mimics did not affect the luciferase activity of MSN-MUT reported gene (Figure 4D). These findings suggest that MSN served as a target for miR-133a-3p, and miR-133a-3p negatively regulated MSN.

### MSN inhibited APS-mediated immunosuppression via maintaining PD-L1 stability

Western blot analysis showed that IFN- $\gamma$  induced MSN expression and phosphorylation, while APS antagonised the effect in a dose-dependent manner (Figure 5A). Co-IP assay analysis indicated that there was interaction between MSN and PD-L1 (Figure 5B). Subsequently, SMMC-7721 and Huh-7 cells were

transfected with sh-MSN#1 and sh-MSN#2 vectors at 48 h for MSN inhibition, and MSN-inhibited SMMC-7721 and Huh-7 cells were treated with cycloheximide (50  $\mu$ g/mL) at 0, 4, 8, 12, 24 h, respectively. Results indicated that PD-L1 expression was promoted by MSN expression in HCC cells (Figure 5C). Finally, wild-type MSN (WT-MSN) and phosphorylated MSN (T558D-MSN) were transfected into treated-SMMC-7721 and Huh-7 cells. Results indicated that IFN- $\gamma$  up-regulated the levels of MSN and PD-L1 proteins in HCC cells, while APS inhibited the levels of MSN and PD-L1 induced by IFN- $\gamma$ . wild type MSN (WT-MSN) and phosphorylated MSN (T558D-MSN) overexpression vector transfection completely restored MSN and PD-L1 levels, while non-phosphorylated MSN (T558A-MSN) overexpression vector only partially restored MSN level (Figure 5D). Besides, wild type MSN (WT-MSN) and phosphorylated MSN (T558D-MSN) overexpression vector transfection completely counteracted the PBMCs-mediated cytotoxicity promoted by APS, while non-phosphorylated MSN (T558A-MSN) overexpression vector only partially counteracted APS promoted-PBMCs-

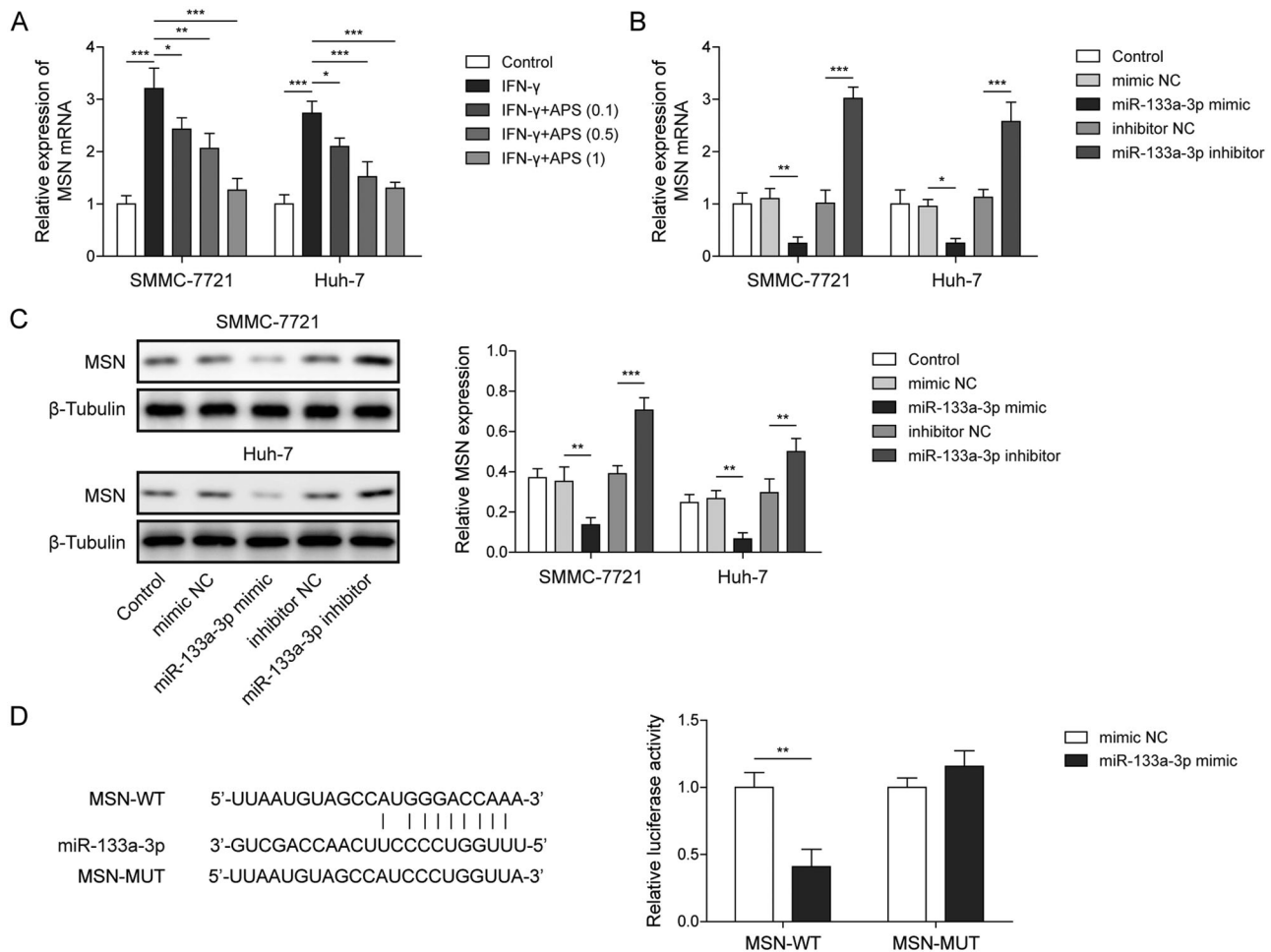


**Figure 4.** MSN served as a target for miR-133a-3p. SMMC-7721 and Huh-7 cells were respectively pre-treated with 0.1 mg/mL, 0.5 mg/mL and 1 mg/mL of APS for 4 h, and APS-treated cells were treated with 10 ng/mL IFN- $\gamma$  for 24 h. (A) The level of MSN was assessed by qRT-PCR. miR-133a-3p inhibitor or miR-133a-3p mimic was transfected into treated SMMC-7721 and Huh-7 cells for miR-133a-3p inhibition or overexpression, NC inhibitor or mimic served as the negative control. (B and C) The level of MSN was assessed by qRT-PCR and Western blot. (D) starBase was used to predict the downstream targets of miR-133a-3p, and the direct binding relationship between miR-133a-3p and MSN was confirmed by dual-luciferase reporter assay. The data were expressed as mean  $\pm$  SD. All data were obtained from at least three replicate experiments ( $n = 3$ ). \* $P < 0.05$ , \*\* $P < 0.01$ , \*\*\* $P < 0.001$ .

mediated cytotoxicity (Figure 5E). These findings suggest that MSN inhibited APS-mediated antitumor effect via maintaining PD-L1 stability.

### APS attenuated PD-L1-mediated immunosuppression via miR-133a-3p/MSN axis

qRT-PCR analysis showed that transfection of miR-133a-3p inhibitor reduced miR-133a-3p level, while transfection of sh-MSN vector has no effect on miR-133a-3p level (Figure 6A). Subsequently, results indicated that IFN- $\gamma$  induced the levels of PD-L1 and MSN proteins in HCC cells, while APS resisted the induction of IFN- $\gamma$  and inhibited the upregulation of PD-L1 and MSN expression. MiR-133a-3p inhibition reversed the inhibitory effect of APS on PD-L1 and MSN, and promote PD-L1 and MSN expression. MSN inhibition resist the effect of miR-133a-3p inhibitor and down-regulate PD-L1 and MSN expression in HCC cells treated with APS and IFN- $\gamma$  (Figure 6B). Furthermore, inhibition of miR-133a-3p counteracted the PBMCs-mediated cytotoxicity promoted by APS, while inhibition of MSN alleviated the effect of miR-133a-3p inhibition and increased PBMCs-mediated cytotoxicity induced by APS and

IFN- $\gamma$  (Figure 6C). These findings suggested that APS attenuated PD-L1-mediated immunosuppression via miR-133a-3p/MSN axis.

### Discussion

Anti-PD-L1 therapy has achieved remarkable clinical results in the treatment of a variety of cancers (Cha et al. 2019; Oba et al. 2020). Our findings indicated that APS attenuated PD-L1-mediated immunosuppression via miR-133a-3p. What's more, MSN served as a target for miR-133a-3p, and MSN promoted immunosuppression via maintaining PD-L1 stability. APS attenuated PD-L1-mediated immunosuppression via miR-133a-3p/MSN axis, which may be the potential mechanism of APS exerts anti-tumor effect in HCC.

APS is a kind of Chinese herbal medicine used as immunosuppressant, which is known as Huang Qi in Chinese. As a powerful immune assistant, APS promotes lymphocyte proliferation in peripheral blood, increases antibody content in serum and enhances cytokine secretion (Chang et al. 2020). Furthermore, the discovery of immune checkpoints is an important breakthrough in cancer treatment. PD-1/PD-L1 is an

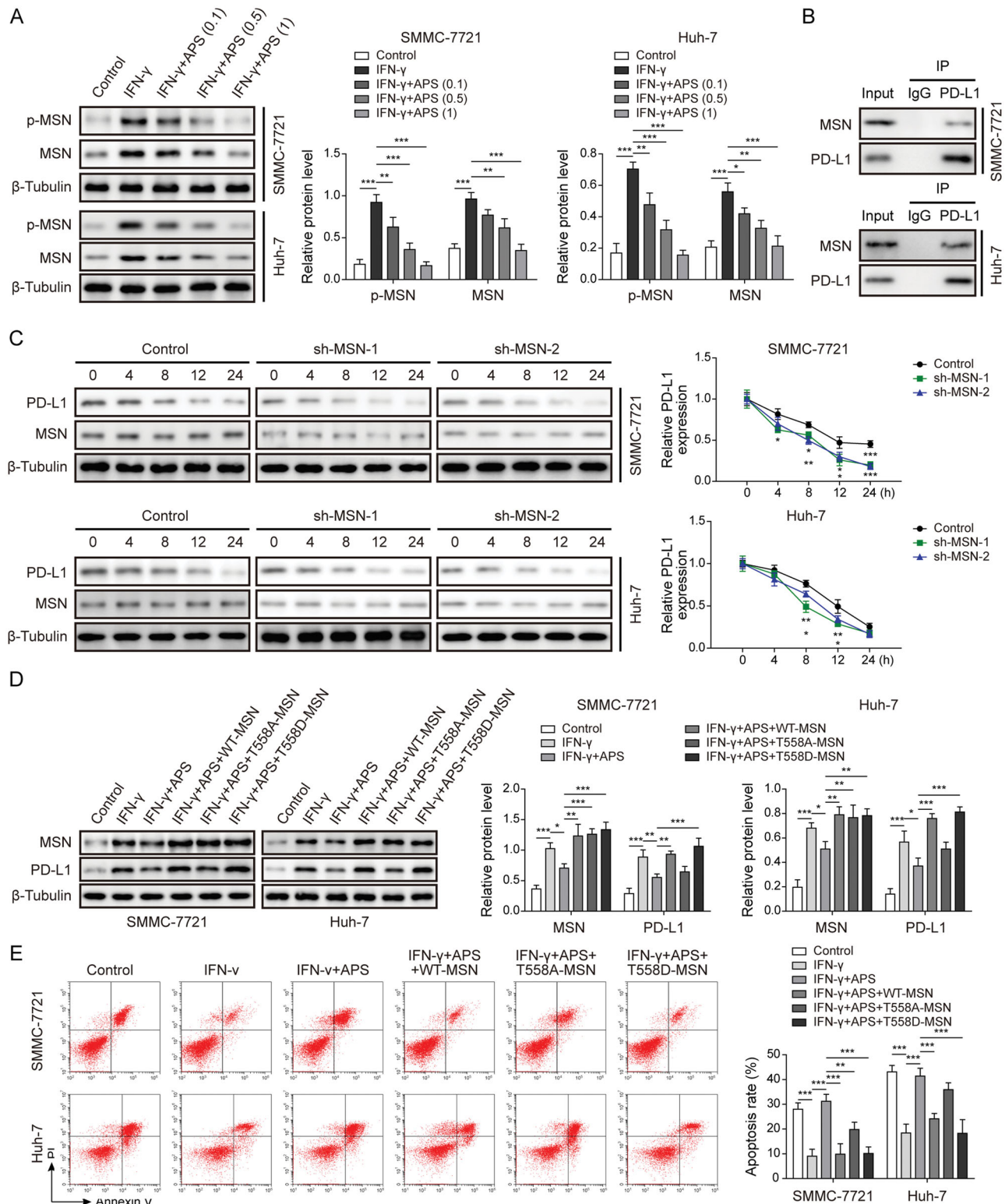


**Figure 5.** MSN inhibited APS-mediated antitumor effect via maintaining PD-L1 stability. SMMC-7721 and Huh-7 cells were respectively pre-treated with 0.1 mg/mL, 0.5 mg/mL and 1 mg/mL of APS for 4 h, and APS-treated cells were treated with 10 ng/mL IFN- $\gamma$  for 24 h. (A) MSN and p-MSN levels were measured by Western blot. (B) The combination of MSN and PD-L1 was verified by co-IP assay. sh-MSN#1 and sh-MSN#2 vectors were transfected into SMMC-7721 and Huh-7 cells at 48 h for MSN inhibition, sh-NC vector served as the negative control, and MSN inhibited SMMC-7721 and Huh-7 cells were treated with cycloheximide (50  $\mu$ g/mL) at 0 h, 4 h, 8 h, 12 h, 24 h. (C) PD-L1 and MSN protein levels were measured by Western blot after MSN inhibition. Treated-SMMC-7721 and Huh-7 cells were transfected with wild type MSN (WT-MSN), non-phosphorylated MSN (T558A-MSN) and phosphorylated MSN (T558D-MSN) vectors. (D) MSN protein level was measured by Western blot. (E) SMMC-7721 and Huh-7 cell apoptosis was evaluated by flow cytometry. The data were expressed as mean  $\pm$  SD. All data were obtained from at least three replicate experiments ( $n = 3$ ). \* $P < 0.05$ , \*\* $P < 0.01$ , \*\*\* $P < 0.001$ .

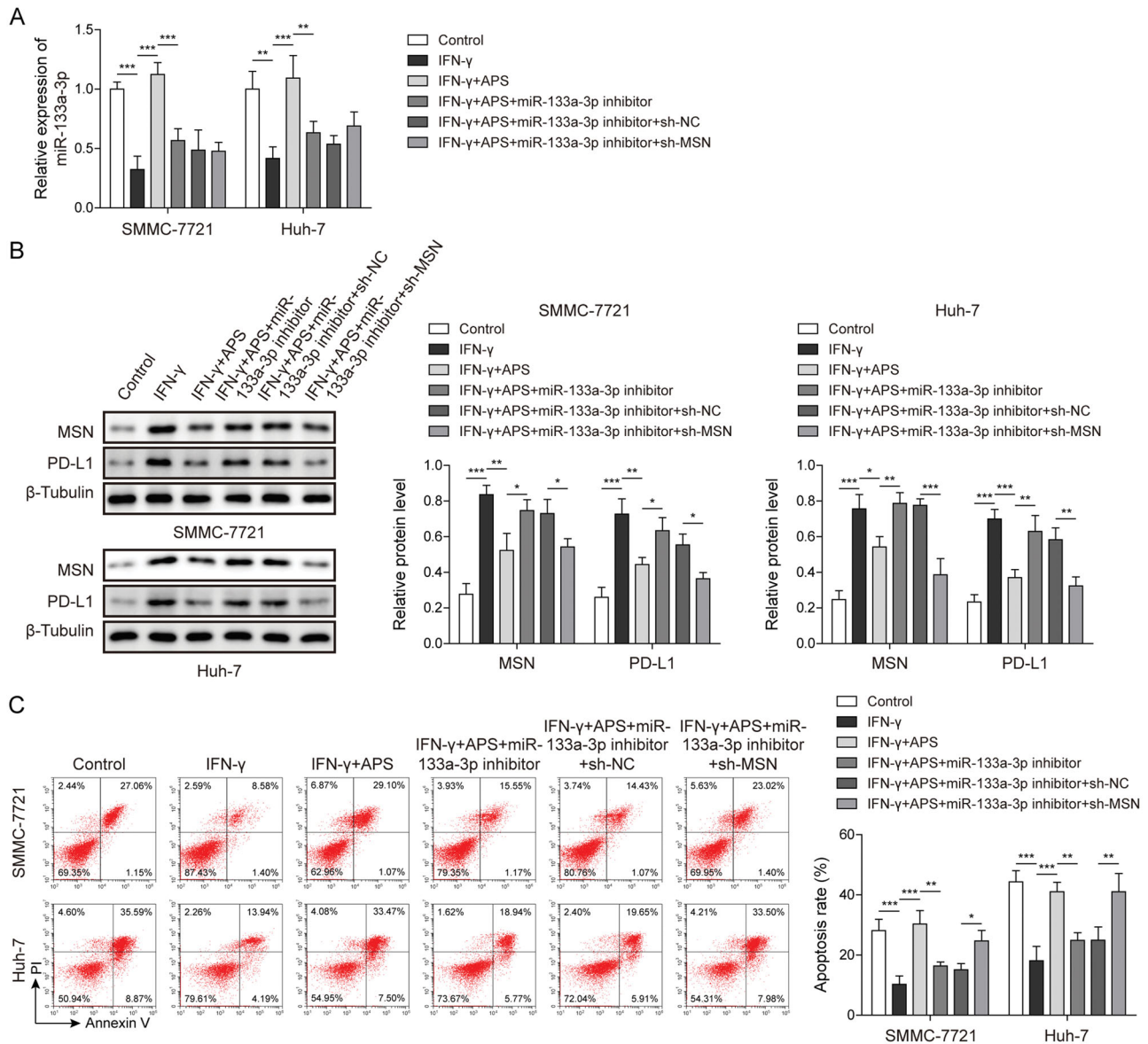


**Figure 6.** APS attenuated PD-L1-mediated immunosuppression via miR-133a-3p/MSN axis. SMMC-7721 and Huh-7 cells were pre-treated with 10 ng/mL IFN- $\gamma$  for 24 h, and then treated with 1 mg/mL of APS for 4 h. The miR-133a-3p inhibitor or sh-MSN was transfected into treated SMMC-7721 and Huh-7 cells (A) miR-133a-3p level was detected by qRT-PCR. (B) The levels of MSN and PD-L1 were measured by Western blot. (C) Activated PBMCs cells were co-cultured with treated SMMC-7721 and Huh-7 cells at 5:1 for 72 h, SMMC-7721 and Huh-7 cells were isolated and collected. SMMC-7721 and Huh-7 cell apoptosis was evaluated by flow cytometry. The data were expressed as mean  $\pm$  SD. All data were obtained from at least three replicate experiments ( $n = 3$ ). \* $p < 0.05$ , \*\* $p < 0.01$ , \*\*\* $p < 0.001$ .

important immune checkpoint, and PD-L1 binds to PD-1 on the surface of immune cells, inducing T cell failure, leading to immunosuppression. Therefore, high expression of PD-L1 contributes to the immune escape of tumour cells (Wu et al. 2019). At present, studies have shown that APS alleviates tumour immunosuppression by reducing PD-L1 expression (Chang et al. 2020). Chang et al. (2020) reported that APS maintains T cell activity and inhibits tumour growth by blocking PD-1/PD-L1 interaction. Our finding showed that APS inhibited tumour growth, down-regulated PD-L1 expression and increased the number of CD8<sup>+</sup> T cells in a dose-dependent manner in HCC. PD-L1 is highly expressed in most tumours, which is induced by IFN- $\gamma$  (Chen et al. 2018). Consistently, our results showed that IFN- $\gamma$  induced PD-L1 expression, and overexpressed-PD-L1 was antagonised by APS in a dose-dependent manner. Furthermore, the highly expressed PD-L1 induced by IFN- $\gamma$  inhibited the HCC cell killing effect mediated by immune cells suggesting high

expression of PD-L1 contributes to immune escape of HCC cells. Whereas, APS increased the rate of apoptosis of HCC cells in a dose-dependent manner, indicating APS may break the immunosuppression mediated by PD-L1.

miRNA was proved to be widely involved in various biological processes. In recent years, the abnormal expression of miRNAs in HCC has received widespread attention (Liang et al. 2018). The antitumor effect of miR-133a-3p in HCC has also been widely reported, Tang et al. (2018) suggested that miR-133a-3p inhibits HCC progression by targeting CORO1C. Our findings indicated that IFN- $\gamma$  inhibited miR-133a-3p expression, but APS alleviated the inhibitory effect of IFN- $\gamma$  in a dose-dependent manner. Inversely, IFN- $\gamma$  induced PD-L1 expression, while APS inhibited the highly expressed PD-L1 in a dose-dependent manner. Further functional studies showed that miR-133a-3p inhibition alleviated the inhibitory effect of APS on PD-L1, and inhibited immune cells mediated-HCC cell killing

effect induced by APS. Namely, APS may break PD-L1-mediated immunosuppression through miR-133a-3p in HCC. miR-133a-3p mainly plays a role in post-transcriptional regulation, which regulates target gene expression by binding to 3'-UTR of mRNA (Zhang et al. 2018). In HCC, MSN served as a target for miR-133a-3p, and miR-133a-3p negatively regulated MSN. MSN plays a key role in many aspects of tumour development, which involves tumour invasion and metastasis, and is a potential biomarker (Hong et al. 2016). Our findings indicated that IFN- $\gamma$  induced MSN expression, while APS antagonised the induction of IFN- $\gamma$  in a dose-dependent manner. What's more, functional research showed that MSN inhibited the antitumor effect of ASP by maintaining the stability of PD-L1. Finally, it is proved that APS affected PD-L1-mediated immunosuppression through the miR-133a-3p/MSN pathway.

## Conclusions

miR-133a-3p played a vital role in PD-L1-mediated immunosuppression by targeting MSN, and MSN inhibited the antitumor effect of ASP by maintaining the stability of PD-L1. APS attenuated PD-L1-mediated immunosuppression via miR-133a-3p/MSN axis. APS may be used as a potential antineoplastic drug, and miR-133a-3p/MSN serves as the potential target. Our research may provide a new direction for the treatment of HCC.

## Acknowledgements

We would like to give our sincere gratitude to the reviewers for their constructive comments.

## Disclosure statement

There are no conflicts of interest to declare.

## Funding

The author(s) reported there is no funding associated with the work featured in this article.

## References

- Akbulut S, Sahin TT, Ince V, Yilmaz S. 2022. Impact of COVID-19 pandemic on clinicopathological features of transplant recipients with hepatocellular carcinoma: a case-control study. *World J Clin Cases*. 10(15):4785–4798.
- Auyeung KK, Han QB, Ko JK. 2016. *Astragalus membranaceus*: a review of its protection against inflammation and gastrointestinal cancers. *Am J Chin Med*. 44(1):1–22.
- Barros FBA, Assao A, Garcia NG, Nonogaki S, Carvalho AL, Soares FA, Kowalski LP, Oliveira DT. 2018. Moesin expression by tumor cells is an unfavorable prognostic biomarker for oral cancer. *BMC Cancer*. 18(1):53–60.
- Baskiran A, Akbulut S, Sahin TT, Koc C, Karakas S, Ince V, Yurdaydin C, Yilmaz S. 2020. Effect of HBV-HDV co-infection on HBV-HCC co-recurrence in patients undergoing living donor liver transplantation. *Hepatol Int*. 14(5):869–880.
- Blank C, Brown I, Peterson AC, Spiotto M, Iwai Y, Honjo T, Gajewski TF. 2004. PD-L1/B7H-1 inhibits the effector phase of tumor rejection by T cell receptor (TCR) transgenic CD8<sup>+</sup> T cells. *Cancer Res*. 64(3):1140–1145.
- Cha JH, Chan LC, Li CW, Hsu JL, Hung MC. 2019. Mechanisms controlling PD-L1 expression in cancer. *Mol Cell*. 76(3):359–370.
- Chang FL, Tsai KC, Lin TY, Yang TW, Lo YN, Chen WC, Chang JH, Lu MK, Chiou CT, Chen PH, et al. 2020. *Astragalus membranaceus*-derived anti-programmed death-1 monoclonal antibodies with immunomodulatory therapeutic effects against tumors. *Biomed Res Int*. 2020:3415471.
- Chen G, Huang AC, Zhang W, Zhang G, Wu M, Xu W, Yu Z, Yang J, Wang B, Sun H, et al. 2018. Exosomal PD-L1 contributes to immunosuppression and is associated with anti-PD-1 response. *Nature*. 560(7718):382–386.
- Chen Y, Chen J, Liu Y, Li S, Huang P. 2015. Plasma miR-15b-5p, miR-338-5p, and miR-764 as biomarkers for hepatocellular carcinoma. *Med Sci Monit*. 21:1864–1871.
- Chen Z, Xie H, Hu M, Huang T, Hu Y, Sang N, Zhao Y. 2020. Recent progress in treatment of hepatocellular carcinoma. *Am J Cancer Res*. 10(9):2993–3036.
- Cristino AS, Nourse J, West RA, Sabdia MB, Law SC, Gunawardana J, Vari F, Mujaj S, Thillaiyampalam G, Snell C, et al. 2019. EBV microRNA-BHRF1-2-5p targets the 3'UTR of immune checkpoint ligands PD-L1 and PD-L2. *Blood*. 134(25):2261–2270.
- Ding L, Lu S, Li Y. 2020. Regulation of PD-1/PD-L1 pathway in cancer by noncoding RNAs. *Pathol Oncol Res*. 26(2):651–663.
- Fehon RG, McClatchey AI, Bretscher A. 2010. Organizing the cell cortex: the role of ERM proteins. *Nat Rev Mol Cell Biol*. 11(4):276–287.
- Han S, Ding X, Wang S, Xu L, Li W, Sun W. 2020. miR-133a-3p regulates hepatocellular carcinoma progression through targeting CORO1C. *Cancer Manag Res*. 12:8685–8693.
- He B, Lin X, Tian F, Yu W, Qiao B. 2018. miR-133a-3p Inhibits oral squamous cell carcinoma (OSCC) proliferation and invasion by suppressing COL1A1. *J Cell Biochem*. 119(1):338–346.
- Hong H, Yu H, Yuan J, Guo C, Cao H, Li W, Xiao C. 2016. MicroRNA-200b impacts breast cancer cell migration and invasion by regulating Ezrin-Radixin-Moesin. *Med Sci Monit*. 22:1946–1952.
- Huang XY, Zhang PF, Wei CY, Peng R, Lu JC, Gao C, Cai JB, Yang X, Fan J, Ke AW, et al. 2020. Circular RNA circMET drives immunosuppression and anti-PD1 therapy resistance in hepatocellular carcinoma via the miR-30-5p/snail/DPP4 axis. *Mol Cancer*. 19(1):92.
- Hwang J, Zhang W, Dhananjay Y, An EK, Kwak M, You S, Lee PC, Jin JO. 2021. *Astragalus membranaceus* polysaccharides potentiate the growth-inhibitory activity of immune checkpoint inhibitors against pulmonary metastatic melanoma in mice. *Int J Biol Macromol*. 182:1292–1300.
- Ince V, Akbulut S, Otan E, Ersan V, Karakas S, Sahin TT, Carr BI, Baskiran A, Samdanci E, Bag HG, et al. 2020. Liver transplantation for hepatocellular carcinoma: Malatya experience and proposals for expanded criteria. *J Gastrointest Cancer*. 51(3):998–1005.
- Kudo M. 2020. Scientific rationale for combined immunotherapy with PD-1/PD-L1 antibodies and VEGF inhibitors in advanced hepatocellular carcinoma. *Cancers*. 12(5):1089.
- Li W, Hu X, Wang S, Jiao Z, Sun T, Liu T, Song K. 2020. Characterization and antitumor bioactivity of *Astragalus* polysaccharides by immunomodulation. *Int J Biol Macromol*. 145:985–997.
- Liang HW, Yang X, Wen DY, Gao L, Zhang XY, Ye ZH, Luo J, Li ZY, He Y, Pang YY, et al. 2018. Utility of miR-133a-3p as a diagnostic indicator for hepatocellular carcinoma: an investigation combined with GEO, TCGA, meta-analysis and bioinformatics. *Mol Med Rep*. 17:1469–1484.
- Liang L, Dong M, Cong K, Chen Y, Ma Z. 2019. Correlations of moesin expression with the pathological stage, nerve infiltration, tumor location and pain severity in patients with pancreatic cancer. *J Buon*. 24:1225–1232.
- Meng F, Su Y, Xu B. 2020. Rho-associated protein kinase-dependent moesin phosphorylation is required for PD-L1 stabilization in breast cancer. *Mol Oncol*. 14(11):2701–2712.
- Nallasamy P, Chava S, Verma SS, Mishra S, Gorantla S, Coulter DW, Byrreddy SN, Batra SK, Gupta SC, Challagundla KB. 2018. PD-L1, inflammation, non-coding RNAs, and neuroblastoma: immuno-oncology perspective. *Semin Cancer Biol*. 52(Pt 2):53–65.
- Oba T, Long MD, Keler T, Marsh HC, Minderman H, Abrams SI, Liu S, Ito F. 2020. Overcoming primary and acquired resistance to anti-PD-L1 therapy by induction and activation of tumor-residing cDC1s. *Nature Comm*. 11(1):5415.
- Qin Y, Chen W, Jiang G, Zhou L, Yang X, Li H, He X, Wang HL, Zhou YB, Huang S, et al. 2020. Interfering MSN-NONO complex-activated CREB signaling serves as a therapeutic strategy for triple-negative breast cancer. *Science Advan*. 6:eaa9960.
- Satilmis B, Sahin TT, Cicek E, Akbulut S, Yilmaz S. 2021. Hepatocellular carcinoma tumor microenvironment and its implications in terms of antitumor immunity: future perspectives for new therapeutics. *J Gastrointest Cancer*. 52(4):1198–1205.
- Spranger S, Spaepen RM, Zha Y, Williams J, Meng Y, Ha TT, Gajewski TF. 2013. Up-regulation of PD-L1, IDO, and T<sup>reg</sup>s in the melanoma tumor microenvironment is driven by CD8<sup>+</sup> T cells. *Sci Transl Med*. 5:200–ra116.

- Tang Y, Pan J, Huang S, Peng X, Zou X, Luo Y, Ren D, Zhang X, Li R, He P, et al. 2018. Downregulation of miR-133a-3p promotes prostate cancer bone metastasis via activating PI3K/AKT signaling. *J Exper Clin Cancer Res.* 37:160.
- Wei J, Li Y, Xu B, Yu J. 2020. *Astragalus* polysaccharides reverse gefitinib resistance by inhibiting mesenchymal transformation in lung adenocarcinoma cells. *Am J Transl Res.* 12(5):1640–1657.
- Wu J, Wang J, Su Q, Ding W, Li T, Yu J, Cao B. 2018. Traditional Chinese medicine *Astragalus* polysaccharide enhanced antitumor effects of the angiogenesis inhibitor apatinib in pancreatic cancer cells on proliferation, invasiveness, and apoptosis. *OTT. ume* 11:2685–2698.
- Wu X, Gu Z, Chen Y, Chen B, Chen W, Weng L, Liu X. 2019. Application of PD-1 blockade in cancer immunotherapy. *Comput Struct Biotechnol J.* 17:661–674.
- Yang S, Sun S, Xu W, Yu B, Wang G, Wang H. 2020. *Astragalus* polysaccharide inhibits breast cancer cell migration and invasion by regulating epithelial-mesenchymal transition via the Wnt/ $\beta$ -catenin signaling pathway. *Mol Med Rep.* 21(4):1819–1832.
- Zhang X, Li Z, Xuan Z, Xu P, Wang W, Chen Z, Wang S, Sun G, Xu J, Xu Z. 2018. Novel role of miR-133a-3p in repressing gastric cancer growth and metastasis via blocking autophagy-mediated glutaminolysis. *J Exper Clin Cancer Res.* 37:320.
- Zhao L, Liu Y, Zhang J, Liu Y, Qi Q. 2019. LncRNA SNHG14/miR-5590-3p/ZEB1 positive feedback loop promoted diffuse large B cell lymphoma progression and immune evasion through regulating PD-1/PD-L1 checkpoint. *Cell Death Dis.* 10(10):731.